Remote Sens. **2015**, *7*, 3526-3547; doi:10.3390/rs70403526

OPEN ACCESS

remote sensing

ISSN 2072-4292

www.mdpi.com/journal/remotesensing

Article

Spectroscopic Remote Sensing of Non-Structural Carbohydrates in Forest Canopies

Gregory P. Asner * and Roberta E. Martin

Department of Global Ecology, Carnegie Institution for Science, 260 Panama Street, Stanford, CA 94305, USA; E-Mail: rmartin@carnegiescience.edu

* Author to whom correspondence should be addressed; E-Mail: gpa@carnegiescience.edu; Tel.: +1-650-325-1521; Fax: +1-650-462-5968.

Academic Editors: Heiko Balzter and Prasad S. Thenkabail

Received: 10 January 2015 / Accepted: 17 March 2015 / Published: 25 March 2015

Abstract: Non-structural carbohydrates (NSC) are products of photosynthesis, and leaf NSC concentration may be a prognostic indicator of climate-change tolerance in woody plants. However, measurement of leaf NSC is prohibitively labor intensive, especially in tropical forests, where foliage is difficult to access and where NSC concentrations vary enormously by species and across environments. Imaging spectroscopy may allow quantitative mapping of leaf NSC, but this possibility remains unproven. We tested the accuracy of NSC remote sensing at leaf, canopy and stand levels using visible-to-shortwave infrared (VSWIR) spectroscopy with partial least squares regression (PLSR) techniques. Leaf-level analyses demonstrated the high precision (R^2 = 0.69–0.73) and accuracy (%RMSE = 13%–14%) of NSC estimates in 6136 live samples taken from 4222 forest canopy species worldwide. The leaf spectral data were combined with a radiative transfer model to simulate the role of canopy structural variability, which led to a reduction in the precision and accuracy of leaf NSC estimation (R^2 = 0.56; %RMSE = 16%). Application of the approach to 79 one-hectare plots in Amazonia using the Carnegie Airborne Observatory VSWIR spectrometer indicated the good precision and accuracy of leaf NSC estimates at the forest stand level (R^2 = 0.49; %RMSE = 9.1%). Spectral analyses indicated strong contributions of the shortwave-IR (1300–2500 nm) region to leaf NSC determination at all scales. We conclude that leaf NSC can be remotely sensed, opening doors to monitoring forest canopy physiological responses to environmental stress and climate change.

Keywords: Carnegie Airborne Observatory; drought tolerance; hyperspectral; imaging spectroscopy; soluble carbon; tropical forest

1. Introduction

Non-structural carbohydrates (NSC) are the mobile portion of a plant's carbon stock, comprised primarily of sugars, starch and pectin [1,2]. Also known as non-structural carbon or soluble carbon, plant NSC are produced and stored in leaves and can be transported to and stored in stems and roots. Plant NSC stocks reflect a balance between carbon fixation via photosynthesis and demand for longer-lasting compounds, such as cellulose and lignin. As such, NSC measurements provide biochemically-based insight into physiological performance (carbon "source") relative to whole plant growth (carbon "sink") [3,4].

NSC are important in trees and other perennial plants, because they provide chemical energy at times of reduced resource availability, such as during dry periods or leaf-off periods in deciduous plants [5]. Recent work reveals that NSC are an important determinant of tree survival during drought [6]. In that study, tropical tree species with inherently low NSC stocks in foliage, stems, and roots were about twice as likely to die in drought compared to those with naturally high NSC stocks. O'Brien *et al.* [6] also found that foliar NSC concentrations mirror those in stems and roots, despite the fact that NSC stocks may be higher in woody tissues compared to foliage [4]. This suggests that leaf NSC can be used as a general diagnostic for plant NSC, at least in a spatial or geographic context. Given the observed and predicted increases in drought frequency and severity in tropical forest regions [7,8], there is a need for studies to determine foliar and whole-plant NSC concentrations as potentially powerful predictors of drought tolerance [9]. This is particularly true in tropical forests, where leaf NSC concentrations display strong phylogenetic and regional variation [10].

The foliage of forest canopies is notoriously difficult to measure at any scale. Tall canopies and complex architectures preclude access and limit field collections to a few leaves or branches per crown. The data resulting from such approaches are challenging to interpret or to scale up and are not often random or systematic samples of an individual tree, a canopy of trees or a landscape [11]. Remote measurement of foliar traits is the only way to accurately sample at stand and ecosystem levels, but remote sensing approaches for NSC estimation have not been broadly developed. Two scales of analysis are needed: (i) leaf-level studies to determine the maximum potential expression of NSC to spectral reflectance and transmittance measurements; and (ii) canopy-level studies to understand if leaf NSC-spectral relationships scale up amidst a background of varying structure (e.g., leaf area index, leaf angle distribution, canopy gaps).

Here, we present a multi-scale analysis establishing the potential for remote measurement of foliar NSC concentrations in forest canopies. We put emphasis on humid tropical and sub-tropical forest canopies, because they exhibit widely varying NSC concentrations [10]. From a remote sensing perspective, we focus on NSC estimation using optical spectroscopy, which provides measurements of leaf reflectance and transmittance, and canopy reflectance, in the 400–2500 nm wavelength range. Spectroscopy has an established history in the detection and analysis of leaf and canopy chemical traits [12,13], but its use for NSC estimation is unproven. From both a theoretical and a laboratory spectroscopy standpoint, remote sensing of foliar NSC should be possible based on the specific wavelength sensitivities of sugars, starch and pectin in the shortwave region of the spectrum [14,15]. Spectral features centered at 1450, 1490, 1510–1580, 1780, 1900, 1960, 2080–2100, and 2270–2280 nm are particularly promising [14], but none or few wavelengths are likely to provide the information needed to predict NSC concentrations accurately. Instead a combination of spectral features, available through full-spectrum chemometric approaches, is likely the best candidate for operational NSC determination at leaf and canopy scales.

2. Methods

2.1. General Approach

We took a three-tier approach to our assessment of NSC from optical spectroscopy (Figure 1). First, we collected leaf reflectance and transmittance spectra (400–2500 nm) in fresh foliage taken from thousands of forest canopies in the field and paired these spectra with laboratory assays of leaf NSC concentration. Second, we combined the leaf spectra with a canopy radiative transfer model that simulates vegetation structural variability and sensor noise and used the simulated canopy reflectance spectra to assess the potential limits of foliar NSC determination at the canopy scale. Finally, we used airborne imaging spectroscopy to assess foliar NSC concentrations at the stand level in forest plots distributed throughout the Amazon basin. For consistency, our leaf and airborne spectral measurements and field-based leaf collections were carried out in the early dry season for each study forest.

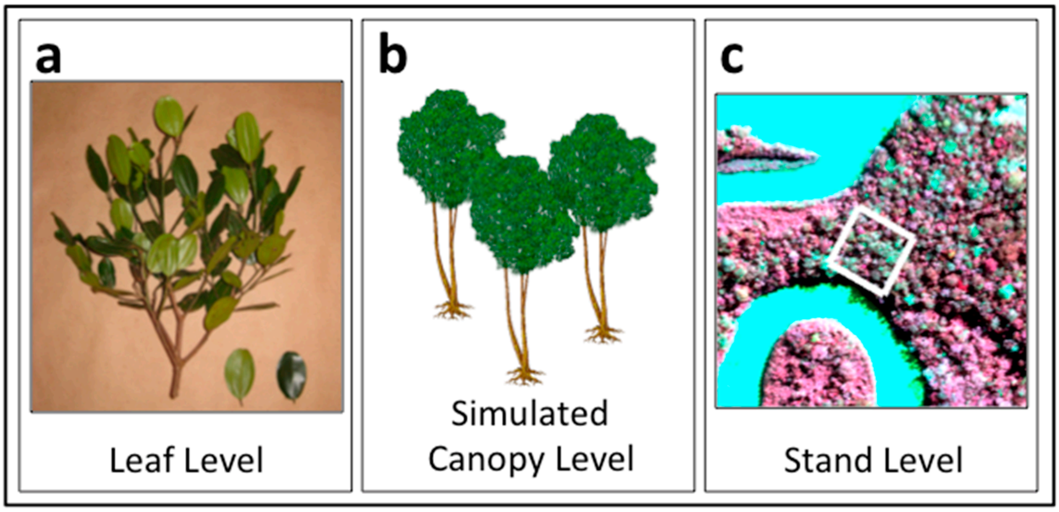

Figure 1. Overview of our three-tier approach to estimate non-structural carbohydrates at (**a**) leaf, (**b**) simulated canopy and (**c**) forest stand scales.

At each of these scales, the chemometric method, called partial least squares regression (PLSR) analysis, as described below, was used to estimate NSC at leaf, modeled-canopy and actual forest stand scales. We developed PLSR-ready datasets for leaves, modeled canopies and real tropical forest field plots using visible-to-shortwave infrared (VSWIR) (400–2500 nm) spectroscopy. These three datasets provided a means to assess the precision and accuracy of NSC determinations from the simplest leaf-level case to the most complex tropical forest stand case.

2.2. Leaf Spectral Properties

A total of 6136 leaf samples representing 4222 different canopy species were collected from 61 sites distributed among tropical and sub-tropical forests in the Amazon Basin, Australia, Borneo, the Caribbean region, Central America, the Hawaiian Islands and Madagascar (Figure 2, Table 1). The global distribution of the samples, and their breakdown into plant families, genera and species, were described in Asner *et al.* [16]. Briefly, the dataset is comprised of the most common plant habits found in tropical forest canopies, including tree (n = 5233), liana (648), palm (74), hemi-epiphyte (109) and vine (51). Across all sites, mean annual temperature (MAT) ranges from 8 to 27 °C, mean annual precipitation (MAP) ranges from 1200 to 6100 mm·yr^{-1} and ground elevation varies from 0 to 3660 m. Soil type varies strongly across sites, from nutrient-poor Oxisols (clays) and Entisols (white sands) to nutrient-rich Inceptisols.

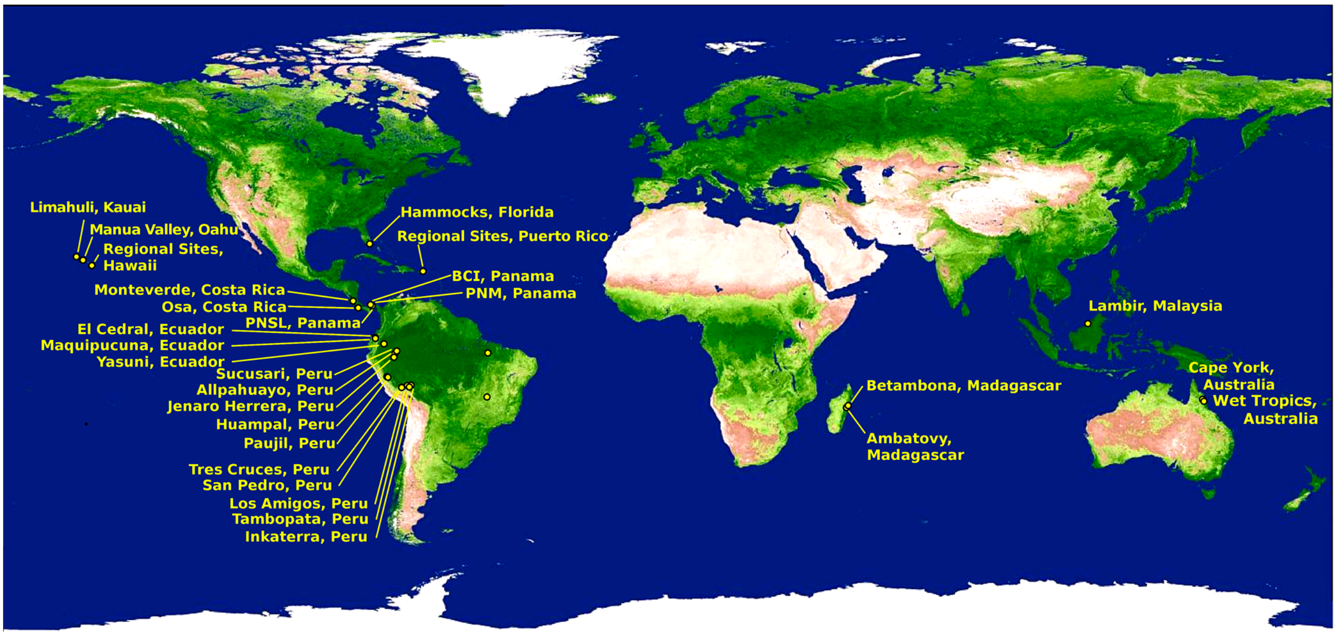

Figure 2. Map of global sampling locations for foliar spectral and non-structural carbohydrates (NSC) in tropical and sub-tropical forest tree canopies. Dots indicate the sites listed in Table 1. Site names BCI, PNM, and PNSL are Barro Colorado Island, Parque Natural Metropolitano, and Parque National San Lorenzo, respectively.

Table 1. Collection sites and taxonomic partitioning of the leaf spectral and NSC dataset.

Political Unit	No. of Sites	Elevation [1] Range	MAP [2] Range	MAT [3] Range	Soil Orders [4]	No. of Samples	No. of Families	No. of Genera	No. of Species
Australia	11	21–1084	1165–3333	18.3–23.7	Alf, Ent, Inc, Oxi, Ult	188	45	121	187
Costa Rica	9	50–1607	2832–4698	17.7–25.8	And, Inc, Ult	746	100	321	607

Table 1. *Cont.*

Political Unit	No. of Sites	Elevation [1] Range	MAP [2] Range	MAT [3] Range	Soil Orders [4]	No. of Samples	No. of Families	No. of Genera	No. of Species
Ecuador	1	1325–1980	3200	18	Inc	242	51	105	162
Hawaii	9	27–1570	1800–5080	13.2–23.8	And, Inc	180	58	129	156
Madagascar	3	330–1118	1700–3020	17–24.3	Ent, Oxi, Ult	624	72	204	426
Panama	4	84–189	1865–3140	26–27.2	Inc	269	65	180	258
Peru	17	92–3660	2380–6128	8–26.6	Ent, His, Inc, Ult	3338	122	515	2090
Puerto Rico	6	140–910	3460–6096	21.3–25.6	Inc, Ult	104	47	86	101
Borneo	1	70–80	2680	26.6	Ult	395	51	108	235

Notes: [1] Elevation (m); [2] MAP = mean annual precipitation (mm); [3] MAT = mean annual temperature (C); [4] soil orders: Alf = Alfisol; And = Andisol; Ent = Entisol; His = Histosol; Inc = Inceptisol; Oxi = Oxisol; Ult = Ultisol.

Hemispherical reflectance and transmittance in the 400–2500-nm wavelength range were measured on six randomly selected fresh leaves immediately after acquiring them from each forest canopy in the field (n = 6136 × 6 = 18,408 reflectance and 18,408 transmittance spectra). The spectral measurements were taken at or close to the mid-point between the main vein and the leaf edge and approximately half way from petiole to leaf tip. The spectra were collected with a field spectrometer (FS-3 with custom detectors and exit slit configurations to maximize signal-to-noise performance; Analytical Spectra Devices, Inc., Boulder, CO USA), an integrating sphere designed for high-resolution spectroscopic measurements and a custom illumination collimator [17]. Twenty-five spectra per sample were averaged and then referenced to a calibration block within the integrating sphere (Spectralon, Labsphere Inc., Durham, NH). An integrating sphere and collimated light source are required to obtain directional-hemispherical reflectance and transmittance measurements, which are subsequently required for use in scaling up to the canopy level with radiative transfer models [18–20]. The high-fidelity measurement capability of our field instruments resulted in leaf spectra that did not require smoothing or other filters commonly used in leaf optical studies.

2.3. Leaf NSC Assays

The method for the chemical determination of leaf NSC was reported by Asner and Martin [21], and the protocol is provided on the Spectranomics website (http://spectranomics.ciw.edu). Briefly, NSC concentration was determined in 0.5 g dry ground leaf tissue through using a neutral detergent fiber (NDF) solution in a fiber analyzer (Model 200/220, Ankom Technology, Macedon, NY, USA). The leaf samples were placed in 1800–1900 mL NDF and agitated for 75 min, then rinsed for 5 min in deionized water. This procedure was repeated three times to ensure maximum removal of NSC. The change in dry mass of the sample, before and after extraction, was used to calculate NSC concentration. Leaf standards were used as references with each digestion to ensure consistency across assays.

2.4. Canopy Reflectance Modeling

We projected the mean leaf reflectance and transmittance spectra (n = 6136 pairs) to the canopy level using the 4SAIL2 (4-Stream Scattering by Arbitrarily Inclined Leaves) radiative transfer model [20]. This model simulates top-of-canopy spectral reflectance based on the measured leaf hemispherical-directional reflectance and transmittance spectra, along with the variation of leaf area index (LAI), leaf angle distribution and other crown geometric-optical properties. For each canopy simulation, a random combination of canopy structural parameters was selected from a very wide range of potential values based on growth-form (e.g., tree, liana), which was combined with the measured leaf spectra, to generate a canopy reflectance signature. Value ranges for each canopy structural parameter are listed in Table 2.

Table 2. Ranges of canopy structural parameters randomly selected during canopy radiative transfer model simulations. LAI = leaf area index; LAD = leaf angle distribution; C_v = crown covering the ground at nadir; Zeta = ratio of crown diameter to tree height. The modeled LAI variation is considered extreme for tropical canopies [22].

Plant Growth-form	LAI	LAD [1]	C_v	Zeta
Trees	2.0–8.0	−0.4 to 0.4 −0.1 to 0.2	0.6–0.8	0.2–0.7
Lianas	1.0–5.0	−0.1 to 0.3 0.3 to 0.6	0.7–0.9	0.1–0.3
Palms	1.0–5.0	−0.8 to −0.2	0.7–0.9	0.1–0.3
Vines	1.0–3.0	−0.1 to 0.3 0.3 to 0.6	0.7–0.9	0.1–0.3
Hemi-epiphytes	2.0–8.0	−0.4 to 0.4 −0.1 to 0.2	0.6–0.8	0.2–0.6

Note: [1] Leaf angle distribution (LAD) is described by a two-parameter model, with the first parameter controlling average leaf inclination and the second parameter controlling the bimodality of the leaf angle distribution [20]. The ranges shown here are extremely wide for tropical vegetation canopies.

These ranges are extreme in most cases, particularly with respect to LAI and leaf angle, both of which do not vary as widely as tested here at spatial resolutions typical of airborne spectroscopy (>1 m). Here, we selected extreme ranges compiled from the literature by Asner *et al.* [23] and Asner and Martin [17] as a means to create possible worst-case scenarios of canopy structure overpowering leaf spectral-chemical variation. Our modeling also included a treatment of both random and systematic spectrometer sensor noise using the technique described by Asner *et al.* [16]. Together, this provided a method to estimate the effects of extreme canopy structural variability and sensor noise on leaf NSC estimation using canopy reflectance in the 400–2500-nm wavelength range. A useful aspect of this approach is that it likely represents the chemical and structural variability of broadleaf forests worldwide.

2.5. Airborne NSC Study

We tested our ability to quantitatively estimate leaf NSC concentrations in actual tropical forest canopies. Airborne imaging spectrometer data were acquired over 79 one-hectare field plots distributed throughout the Peruvian Amazon using the Carnegie Airborne Observatory (CAO) (Figure 3), which includes a high-fidelity VSWIR imaging spectrometer [24]. In each field plot, multiple full-sunlight canopies were selected for leaf collections (n = 3–38 per plot) as described in detail by Asner *et al.* [11]. Foliage from these canopies was assayed for NSC using the same technique described earlier for the global leaf collection. The field-collected NSC data were averaged to the plot level.

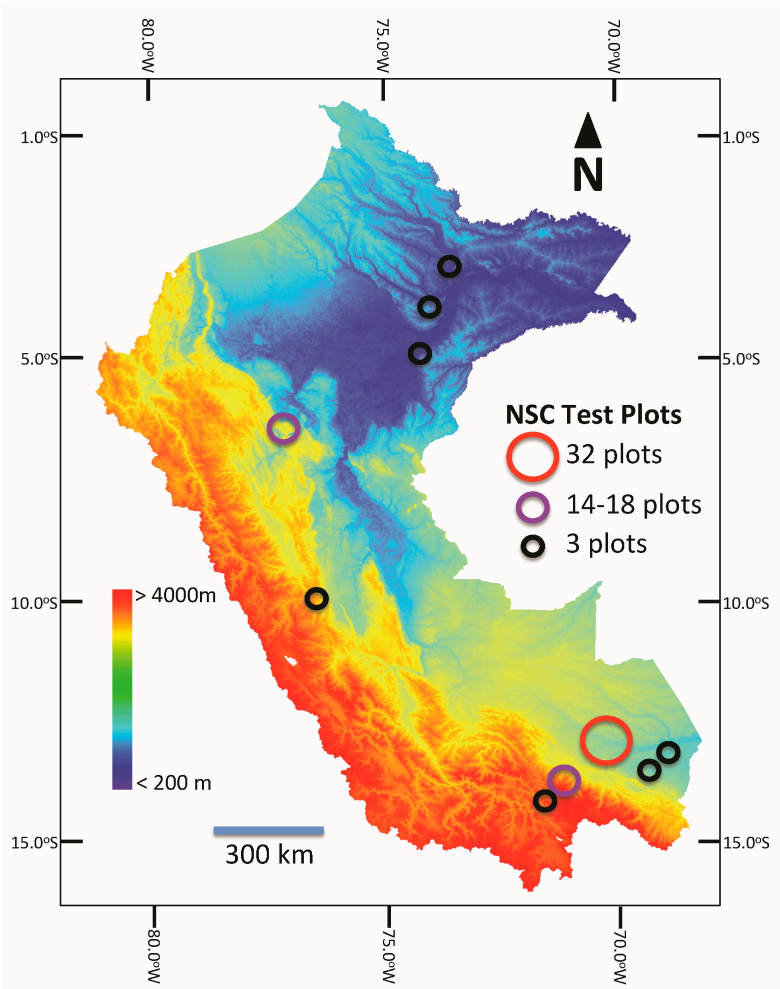

Figure 3. The regional distribution of one-hectare field plots in the Amazon basin and Andean forests of Peru. The map is a digital elevation model (DEM) of Peru derived from NASA Shuttle Radar Topography Mission (SRTM) data. Circles contain clusters of field plots as indicated and are arrayed geographically to maximize environmental and floristic variation as reported by Asner *et al.* [11].

The VSWIR data were collected over each field plot from an altitude of 2000 m above ground level (a.g.l.), an average flight speed of 55–60 m s^{-1} and a mapping swath of 1200 m. The VSWIR spectrometer measures spectral radiance in 480 channels spanning the 252–2648 nm wavelength range in 5-nm increments (full-width at half-maximum). The spectrometer has a 34° field-of-view and an instantaneous field-of-view of 1 mrad. At 2000 m a.g.l., the VSWIR data collection provided a 2.0-m ground sampling distance, or pixel size, throughout each study landscape. The VSWIR data were radiometrically corrected from raw DN values to radiance (W sr^{-1} m^{-2}) using a flat-field correction, radiometric calibration coefficients and spectral calibration data collected in the laboratory. The image data were atmospherically corrected from radiance to apparent surface reflectance using the ACORN-5 (Atmospheric Correction Now) model (Imspec LLC, Glendale, CA USA). The reflectance imagery was corrected for cross-track brightness gradients using a bidirectional reflectance distribution function (BRDF) modeling approach described by Colgan *et al.* [25]. The sunlit portions of canopies in each 1-ha plot were filtered and averaged based on the method described by Asner *et al.* (2015). This method removes pixels unsuitable for sunlit canopy spectroscopic measurement, including non-canopy surfaces (bare ground), shaded canopy pixels and pixels with low foliar content. To achieve this, we use a LiDAR (light detection and ranging) scanner flown with the spectrometer to estimate the height of the vegetation at a resolution of 8 laser shots per VSWIR spectral pixel and to model inter-canopy shade (Asner *et al.*, 2015). To ensure that remaining candidate spectral pixels have sufficient foliar content, we apply a minimum NDVI threshold of 0.8. Spectral pixels that pass this combination of filters are considered suitable for NSC analysis at a mapping resolution of 1 ha. The resulting average reflectance spectrum of each 1-ha field plot was trimmed at the far ends (<400 nm, >2450 nm) of the measured wavelength range, as well as in regions dominated by atmospheric water vapor (1350–1480, 1780–2032 nm). Water vapor features preclude the use of these wavelength regions in canopy chemical analyses.

2.6. Chemometric Analyses

We used PLSR analysis [26] to characterize the strength of NSC expression in the spectroscopy of leaves, modeled canopies and actual canopies at the stand level. Leaf reflectance and transmittance were each tested using the field-based measurements followed by re-sampling to the 10-nm full-width half-maximum bandwidth spanning the 400–2500 nm spectral range and averaging of six individual leaf measurements (n = 6136 leaf samples). Canopy reflectance (n = 6136 simulated canopies) was tested in a similar configuration, but with the 1330–1430-nm and 1760–2030-nm atmospheric water vapor regions removed from the simulated VSWIR data [27]. Actual forest stand data (n = 79 field plots) from the Amazon were treated the same way.

For all PLSR analyses, we minimized statistical overfitting by utilizing the prediction residual error sum of squares (PRESS) statistic [28]. The PRESS statistic was calculated through a cross-validation prediction for each PLSR model. This cross-validation procedure iteratively generates regression models while reserving a portion of the samples (10% for input datasets with >100 samples; leave-one-out for <100 input samples) from the input dataset until the root mean square error (RMSE) for the PRESS statistic is minimized. The leaf and modeled canopy datasets were each randomly divided into 40 subsets to generate 40 unique PLSR models containing approximately 150 samples each. For the measured stand-level reflectance data, 70% were randomly selected on an iterative basis to generate 1000 PLSR models. For each subset (leaf and modeled canopy) or iteration (stand level) in this evaluation, PLSR weighting coefficients derived for each spectral band were multiplied by the spectral values to generate predictions of NSC concentration. This provided a way to calculate the variation in the calibration predictions of NSC concentrations from each dataset. Statistics were computed for the PLSR equations resulting in robust models (R^2 > the mean of the 40 or 1000 iterations at the leaf and modeled canopy or actual canopy, respectively) to assess the precision and accuracy of NSC remote sensing with spectroscopy. The coefficient of determination (R^2) was used as the metric of PLSR model precision and the RMSE as an assessment of the model accuracy. The mean PLSR weighting coefficients are provided in Appendix Table A1.

3. Results

3.1. Leaf-Level Performance

The global compilation of leaf reflectance and transmittance spectra indicated very wide-ranging values at nearly all wavelengths (Figure 4). Maximum reflectance variation occurred in the near-infrared (IR) and shortwave-IR between 800 and 1800 nm. For leaf transmittance, maximum variation occurred in the shortwave-IR from 1500–2450 nm. The variation expressed in these spectra meets or exceeds the variation reported for leaf optical properties in other biomes [29–34] and matches the reported variability achieved in models of leaf optical properties [19,35]. This suggests that our leaf optical database is globally relevant.

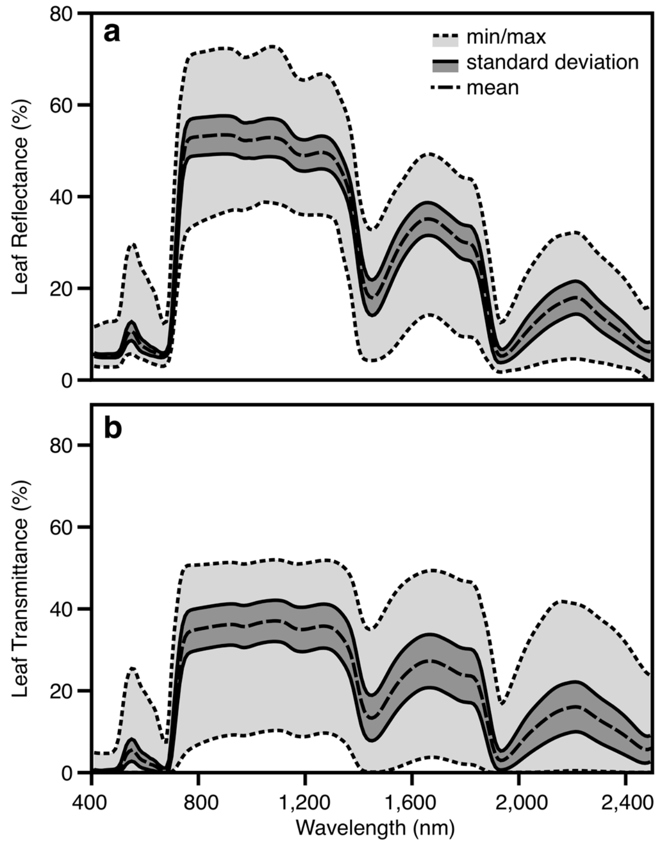

Figure 4. Leaf-level (**a**) reflectance and (**b**) transmittance spectra of fresh (live) samples collected from 6136 forest canopy growth-forms in sub-tropical and tropical forests worldwide. The locations of the sample collections are shown in Figure 2, and the general site information is provided in Table 1. The thick dashed line indicates mean values; dark grey areas indicate one standard deviation; light grey areas indicate the total range of values.

Chemical analyses of the 6136 leaf samples indicated extremely wide-ranging concentrations of NSC, from 16.5% to 84.5% of total leaf mass (Table 3). Parallel to the spectra, this NSC range approximately meets the range reported for live, fresh foliar material worldwide [1,5,9]. Based on this range of chemical values, the PLSR analyses indicated that NSC can be estimated at the leaf level from reflectance with high precision (mean R^2 = 0.73 ± 0.06) and accuracy (average %RMSE = 12.9%) (Table 3). Transmittance-based results showed similar performance, with mean R^2 = 0.69 ± 0.03 and average %RMSE = 13.9%. Analysis of sub-regional leaf datasets, such as from the Amazon basin (Table 1), indicated similar performance levels. Spectral weightings from the PLSR models with the largest deviations from zero (positive or negative) indicate that the shortwave-IR (2000–2450 nm) and, to a slightly lesser extent, the 1300–1800 nm region, were most critical to the determination of NSC concentrations from leaf reflectance and transmittance (Figure 5a,b). PLSR spectral weights are derived from matrix multiplication that simultaneously takes into account spectral variation relative to changing chemical concentration. In Figure 5, departures from zero indicate the increasing importance of spectral features in determining a chemical concentration [36]. The most important features align with known centers of NSC expression in the spectrum, particularly from 1450 to 2270 nm, as detailed by Curran [14].

Table 3. Calibration performances for non-structural carbohydrates (NSC) derived from optical spectroscopy in the 400–2450-nm wavelength range at leaf, simulated crown and forest stand levels. Mean ± standard deviation values are presented with minimum and maximum values in parentheses. RMSE = root mean squared error; %RMSE is standardized to the mean value. Vectors indicate the number of spectral dimensions selected by the partial least squares regression (PLSR) analyses to achieve the reported precision (R^2) and accuracy (RMSE) results. The range of vector numbers indicates variation among repeated PLSR model runs. For leaf reflectance and transmittance, as well as canopy reflectance, total n = 6136; these samples were randomly partitioned into 40 sub-samples with n_{sub} = 150 for iterative PLSR analyses. For stand-level reflectance, n = 79; these samples were randomly partitioned into 1000 sub-samples with n_{sub} = 55 for iterative PLSR analyses.

Approach	Chemical Range	R^2	RMSE	%RMSE	Vectors
Leaf reflectance	16.2–84.5	0.73 ± 0.06	5.9 ± 0.8	12.9; (9.1–15.6)	24; (20–38)
Leaf transmittance	16.2–84.5	0.69 ± 0.03	6.4 ± 0.5	13.9; (12.5–15.9)	21; (17–26)
Canopy reflectance	16.2–84.5	0.56 ± 0.09	7.4 ± 0.90	16.1; (11.4–19.4)	13; (9–19)
Stand reflectance	36.0–71.9	0.49 ± 0.14	4.4 ± 0.87	9.1; (9.2–12.6)	4; (3–12)

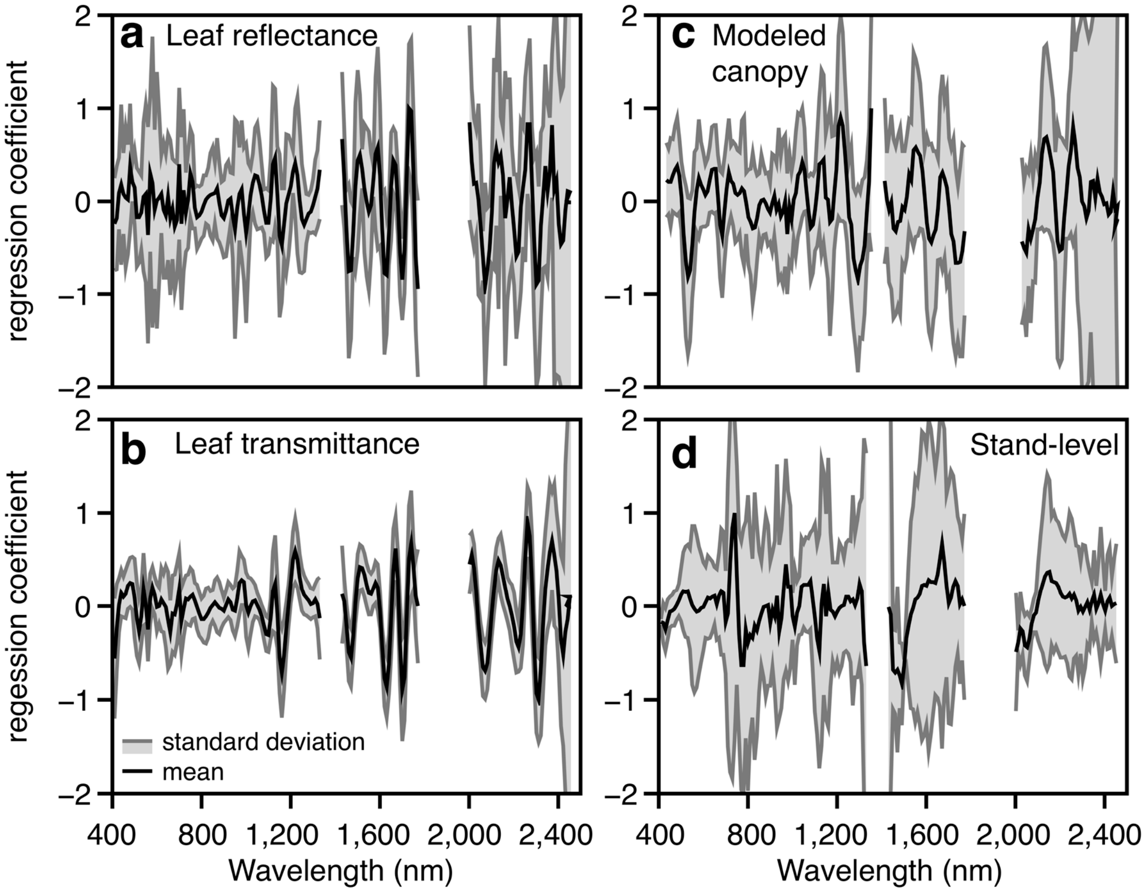

Figure 5. PLSR spectral weighting factors for NSC estimation in foliage at three scales: (**a**) leaf reflectance and (**b**) transmittance; (**c**) modeled canopy reflectance; and (**d**) actual forest stand-level reflectance. In each panel, the black line indicates the mean values, and the grey shading indicates one standard deviation among PLSR models run iteratively on random subsets of samples from each leaf, canopy and stand-level database.

3.2. Canopy-Level Performance

Canopy simulations using the leaf reflectance and transmittance dataset (Figure 4) integrated with variable canopy structure and sensor noise resulted in an extremely wide range of canopy reflectance (Figure 6a), relative to actual stand-level canopy observations (Figure 6b). Maximum reflectance variation was observed in the near-IR (800–1300 nm) and secondarily in the shortwave-IR between 1500 and 1800 nm. The extreme structural variation incorporated into the modeled spectra reduced the precision (mean R^2 = 0.56 ± 0.09) and accuracy (avg. %RMSE = 16.1%) of foliar NSC estimates, as compared to leaf-level results (Table 3). Spectral PLSR weightings also shifted at the canopy scale, with the maximum signal for NSC estimates expressed in the 1200–2300 nm wavelength ranges (Figure 5c).

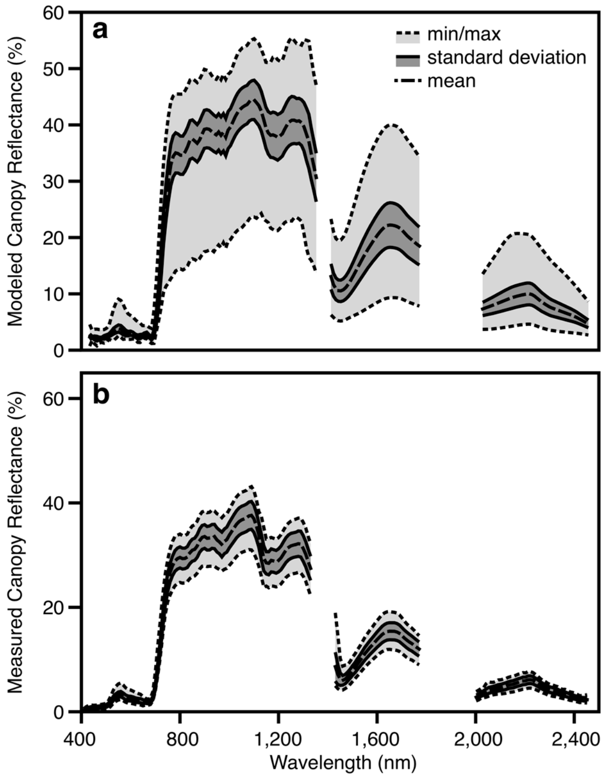

Figure 6. (**a**) Simulated canopy reflectance calculated using all leaf spectra (Figure 4) with a canopy radiative transfer model and a random selection of canopy structural properties (Table 2). (**b**) Actual forest stand-level reflectance spectra from 79 one-hectare field plots in the Amazon basin. The thick dashed line indicates mean values; dark grey areas indicate one standard deviation; light grey areas indicate the total range of values.

3.3. Airborne Imaging Spectroscopy

Airborne imaging spectroscopy of the 79 one-hectare plots showed much less spectral variability compared to the simulated canopies (Figure 6b). This was expected given the approach of automated averaging of spectra pre-filtered and selected for sunlit, highly foliated portions of canopies in each field plot [11]. Moreover, actual stand-level spectral data were of somewhat lower overall reflectance in the near-IR as compared to the simulated canopy-level spectral data. This is caused by within-canopy shading, which is present in the real data and absent in the simulations. Despite these differences, similar to the canopy simulations, we found that maximum stand-level reflectance variation was expressed in the near-IR (800–1300 nm) and secondarily in the shortwave-IR from 1500–1800 nm. PLSR analyses of the filtered airborne spectra against leaf NSC samples taken from the field plots indicated good precision (mean $R^2 = 0.49 \pm 0.14$) and excellent accuracy (average %RMSE = 9.1%) (Table 3). Whereas precision declined slightly in comparison to leaf-level NSC retrievals, the error (RMSE, %RMSE) decreased relative to the canopy-scale simulations. This results from the averaging of spectra and leaf samples within each field plot, compared to a very liberal use of canopy structural variation to the modeled spectra (Table 2). Spectral PLSR weightings indicated the importance of the 700- to 720-nm range ("red-edge") and the shortwave-IR (1500–2300 nm) in determining foliar NSC concentrations at this ecological scale (Figure 5d).

4. Discussion

Using a three-tier strategy, we determined that leaf NSC concentrations can be estimated using high-fidelity spectroscopy at leaf, canopy and whole-stand scales with demonstrably high precision and accuracy compared to laboratory-based chemical assays. Laboratory wet-chemical assays of NSC typically result in relative errors of about 9% on a per sample basis [37], and our lab sampling protocols result in a similar error level. Leaf-level spectroscopy yielded relative errors ranging from just 13%–14% (Table 3). When averaging samples and spectral signatures at the forest-stand level, relative uncertainties were reduced to about 9%. From either ecological or chemometric standpoints, the spectral- and wet chemical-based approaches are nearly indistinguishable.

Our model-based results should be considered quite liberal in the context of canopy structural variation, serving as a contributor to canopy reflectance. We varied LAI from 1.0 to 8.0 units (Table 2), which not only incorporates a global range of LAI values [23], but is also far more variable than what is typically encountered in closed-canopy tropical forests [38]. Our leaf angle distributions and other model parameters were also structurally very wide ranging [18,20]. Surprisingly, we found that leaf NSC estimates from modeled canopy spectroscopy remained demonstrably good, although precision and accuracy did suffer under such extreme canopy structural variability compared to the leaf-level analyses. This is important because, although past studies highlight the potential use of spectroscopy for canopy chemical trait analysis [13,14,39], other studies have emphasized the potentially dominant role of canopy structure over chemistry in determining canopy spectral reflectance [40]. Here, we found insufficient evidence to suggest that structural variability in forest canopies will critically impair NSC estimation from imaging spectroscopy.

An additional finding was that the portions of the reflectance spectrum responsible for NSC determinations shifted in wavelength when going from leaf to canopy and stand levels (Figure 5). Whereas the shortwave-IR between 1300 and 2500 nm was almost uniformly important to NSC estimation at the leaf level, canopy-scale estimates were shifted to shorter wavelengths (closer to 1200 nm). This is caused by increased absorption at the canopy level, which is related to increased leaf area index [17,19]. The leftward shift of the PLSR weightings was more pronounced at the stand level, where the spectral red-edge (~750 nm) was a co-predictor of NSC, in addition to spectral features in the shortwave-IR. This too is caused by canopy-scale absorption. Finally, we note that most of the PLSR weighting "peaks" (departures from zero to negative or positive values; Figure 5) are in line with many of the NSC-related features first suggested by Curran [14]. This suggests consistency in the expression of foliar NSC in leaf and canopy reflectance spectra.

The total carbon content of a leaf is approximately equal to the sum of NSC, cellulose, hemi-cellulose and lignin [41]. One might therefore predict that remote sensing of NSC is somehow inversely related to remote estimation of the other carbon molecules, and indeed, lignin and cellulose have long been a focus of imaging spectroscopy [12,39]. In a previous study, we found that the spectral reflectance features associated with NSC were anti-correlated with spectral features expressed by lignin ($r = -0.64$) and cellulose ($r = -0.77$; $p < 0.01$) [11]. This internal consistency in the diversity of spectral expression among major leaf carbon constituents suggests that all three sets of compounds can be estimated from VSWIR imaging spectroscopy. If so, this will open new doors to large-scale ecological studies of multiple carbon fractions in the foliage of forest canopies. The resulting data could, in turn, be used to estimate the relative strength of carbon sources (photosynthesis) and sinks (growth; tissue allocation) at ecological scales unobtainable using field and laboratory sampling alone. The dynamics of these environmentally-responsive carbon pools will be a focus of forthcoming studies with airborne high-fidelity imaging spectroscopy from the Carnegie Airborne Observatory.

Remote sensing of foliar NSC will allow for measurement and monitoring of the direct products of photosynthesis in forest canopies at an ecological scale never before achieved. This will facilitate large-scale assessments of forest canopy responses to changes in multiple environmental factors, including climate. Drought and temperature tolerance are critically important applications of NSC remote sensing with spectroscopy. With the future promise of global imaging spectroscopy via Germany's EnMap (Environmental Mapping and Analysis Program) and NASA's HyspIRI (Hyperspectral Infrared Imager) missions, climate change effects on forest canopy NSC concentrations will, for the first time, be mapped and placed in an Earth system context. Until then, airborne imaging spectrometers will be the best way forward to understand NSC dynamics at landscape to regional scales, as well as at the scale of individual canopies and species. The spectroscopy of leaf NSC is a gateway to developing a chemical basis for remote sensing of forest physiology at the macroscale.

5. Conclusions

Remote sensing of leaf non-structural carbohydrates (NSC) may provide a spatially-explicit understanding of forest canopy exposure or susceptibility to increasing temperatures, decreasing precipitation and other climate perturbations. Using a global dataset of leaf chemical and spectral properties in tropical forests, we found that leaf NSC concentrations in 6136 plants can be estimated with high precision (R^2 = 0.69–0.73) and accuracy (%RMSE = 13%–14%). Incorporating leaf spectral data into a radiative transfer model resulted in a reduction in the precision and accuracy of leaf NSC estimation at the canopy level (R^2 = 0.56; %RMSE = 16%). However, application of imaging spectroscopy to 79 one-hectare plots in Amazonia indicated the good precision and accuracy of leaf NSC estimates at the forest stand level (R^2 = 0.49; %RMSE = 9.1%). Spectral analyses indicated strong contributions of the shortwave-IR (1300–2500 nm) region to leaf NSC determination at all scales. These remotely-sensed estimates of NSC are indistinguishable, in terms of precision and accuracy, from those made via laboratory assay and can now be carried out at ecological scales otherwise intractable via ground- and laboratory-based studies. Future airborne and satellite-based spectrometers should be designed to deliver high-quality spectra, such as those used in this study, in order to advance NSC mapping for studies of biospheric responses to climate change.

Acknowledgments

We thank the Spectranomics team for field, laboratory, modeling and remote sensing assistance. This study and the Spectranomics Project are supported by the John D. and Catherine T. MacArthur Foundation. The Carnegie Airborne Observatory is made possible by the Gordon and Betty Moore Foundation, the John D. and Catherine T. MacArthur Foundation, Avatar Alliance Foundation, W. M. Keck Foundation, the Margaret A. Cargill Foundation, Grantham Foundation for the Protection of the Environment, Mary Anne Nyburg Baker and G. Leonard Baker Jr., and William R. Hearst III.

Author Contributions

Gregory Asner and Roberta Martin designed the research, collected the field data, carried out the modeling and statistical analyses and wrote the paper.

Conflicts of Interest

The authors declare no conflict of interest.

Appendix

Table A1. PLSR Weightings for Non-structural Carbohydrates (NSC) in Forest Leaves and Canopies.

Leaf Level			Modeled Canopy		Measured Stand-Level Canopy	
Wavelength	**Leaf Reflectance**	**Leaf Tranmittance**	**Wavelength**	**Canopy Reflectance**	**Wavelength**	**Canopy Reflectance**
Intercept	43.92346158	44.09943433	*Intercept*	49.56582227	*Intercept*	−154.9237312
409.68	−371.3165126	−919.2181631	*433.67*	−133.9772842	*409.31*	−378.8371125
419.68	−228.6673269	−529.911383	*443.36*	69.28851678	*419.33*	−323.278948
429.69	56.99304407	−135.8144438	*453.06*	64.55473098	*429.34*	−364.7098297
439.70	252.1839902	366.6273342	*462.76*	91.50801732	*439.36*	−236.7114492
449.70	151.0924843	136.6963453	*472.47*	119.5154075	*449.37*	−55.19831014
459.71	383.5269807	484.0310369	*482.18*	150.4002381	*459.39*	15.85640461
469.72	−532.7811941	545.345442	*491.90*	234.7742488	*469.40*	78.62211678
479.72	874.8150235	350.917737	*501.62*	86.41842172	*479.42*	120.5855001
489.73	822.4099553	173.4894125	*511.35*	8.246857264	*489.43*	175.8115229
499.74	−175.7833749	27.35911747	*521.08*	−189.3421036	*499.45*	220.9395279
509.74	−317.9762259	−192.7788036	*530.81*	−269.1251103	*509.46*	210.191244
519.75	−306.0900255	−431.1836785	*540.55*	−274.2991826	*519.48*	150.6738296
529.76	−167.351235	−240.2814429	*550.29*	−123.6322331	*529.49*	101.5254057
539.76	143.9138163	395.8328311	*560.04*	92.04892792	*539.51*	76.44952998
549.77	374.1549401	57.48124938	*569.79*	94.54929241	*549.52*	45.34680455
559.78	−1061.982882	−604.6443121	*579.55*	208.2648986	*559.54*	25.00890073
569.78	322.4597226	81.14812637	*589.31*	134.7526353	*569.55*	24.16803965
579.79	1097.252175	451.6732106	*599.08*	66.2640756	*579.57*	47.18824022
589.80	245.0388146	408.9186842	*608.85*	−55.51377327	*589.58*	83.08167905
599.80	−607.0770945	48.72887079	*618.62*	−75.85092513	*599.60*	82.39917972
609.81	−378.816813	−56.99428184	*628.40*	−17.03735391	*609.61*	128.3267049
619.82	97.75052815	59.77830425	*638.18*	−32.12081198	*619.63*	173.778067
629.82	−106.6153207	−9.505604153	*647.97*	−50.92780089	*629.64*	195.5438373
639.83	14.72573507	−92.36009547	*655.29*	11.62208161	*639.66*	214.9546168
649.84	297.9863014	−197.5296171	*665.09*	−27.56064832	*649.67*	260.5694842
659.84	−303.162915	−556.6519505	*674.90*	−15.65527363	*659.69*	−58.72666144
669.85	−344.4751678	−155.9677424	*684.69*	−14.97514638	*669.70*	−11.59788135
679.86	−497.4206742	75.52539134	*694.48*	−40.57359288	*679.72*	−170.2091699
689.86	−269.2332816	−67.23979032	*704.27*	−12.59050278	*689.73*	−247.522385

Table A1. *Cont.*

Leaf Level			Modeled Canopy		Measured Stand-Level Canopy	
Wavelength	**Leaf Reflectance**	**Leaf Tranmittance**	**Wavelength**	**Canopy Reflectance**	**Wavelength**	**Canopy Reflectance**
699.87	656.962502	348.9920474	*714.05*	54.56084237	*699.75*	−239.705834
709.88	−435.3464835	−285.6378627	*723.83*	83.71100952	*709.76*	−136.6003647
719.88	223.2205287	−84.4375331	*733.60*	45.40445656	*719.78*	−45.58251118
729.89	−87.0258821	191.5929311	*743.36*	58.55044007	*729.79*	2.736042706
739.90	−192.0743113	100.6395645	*753.12*	−8.086347346	*739.81*	66.49776933
749.90	477.7664756	116.8965368	*762.88*	−53.38093568	*749.82*	37.1632202
759.91	644.2351532	251.9308119	*772.63*	12.60744724	*759.84*	−29.33069299
769.92	91.44899258	220.1083154	*782.37*	118.8497702	*769.85*	−63.95888037
779.92	−479.0475033	46.04921125	*792.11*	37.4712146	*779.87*	−74.93098304
789.93	−529.3763639	−184.3764745	*801.85*	−86.76430524	*789.88*	−46.20603431
799.94	−391.9987476	−374.1086586	*811.58*	−112.3232265	*799.90*	−51.7597739
809.94	−129.0286866	−361.8888455	*821.30*	−126.9358054	*809.91*	−46.18316548
819.95	196.9461251	−256.366572	*831.02*	11.19585641	*819.93*	−43.22734258
829.96	216.9529804	−45.80192762	*840.73*	53.78026185	*829.94*	−19.5644525
839.96	304.8075438	26.02803471	*850.44*	57.35391261	*839.96*	−11.34007976
849.97	197.7626744	84.80551186	*860.14*	−76.66158364	*849.97*	−16.3196782
859.97	82.57576874	158.8608747	*869.84*	−2.719827379	*859.99*	5.129842753
869.98	45.5682532	45.63869203	*879.53*	−12.98552828	*870.00*	12.42068434
879.99	−80.14214218	−94.3029056	*889.22*	6.764800803	*880.02*	−12.93440156
889.99	−181.6138235	−96.67063657	*898.90*	8.280011119	*890.03*	−9.43695131
900.00	−171.5954815	−83.31427284	*908.58*	22.72116524	*900.05*	−24.87391216
910.01	−64.81621826	53.6327811	*918.25*	−99.07303695	*910.06*	44.69227182
920.01	−31.55516956	211.7780901	*927.92*	−45.43664117	*920.08*	123.1759786
930.02	196.1039688	21.82398383	*937.58*	−49.45697949	*930.09*	−4.909074581
940.03	−163.795639	−255.7551743	*947.23*	−31.80894597	*940.11*	12.09910326
950.03	−706.7859755	−377.7214634	*956.88*	−37.39552131	*950.12*	259.5361108
960.04	−293.5590555	−63.5208901	*966.53*	−38.20602646	*960.14*	217.2184419
970.05	−388.6215367	689.0111029	*976.17*	-36.7076795	*970.15*	224.4095154
980.05	538.40279	810.433792	*985.81*	19.09113554	*980.17*	268.1602899
990.06	50.519203	696.985289	*995.44*	73.0029157	*990.18*	312.1828414
1000.07	−421.9882309	−230.8351216	*1005.06*	−29.84729617	*1000.20*	−104.5367656
1010.07	−269.1901213	−358.8756365	*1014.68*	−115.5968899	*1010.21*	−188.2529108
1020.08	−117.813784	−89.79630257	*1024.29*	−21.97010843	*1020.23*	17.75207205
1030.09	234.8164256	142.6136904	*1033.90*	61.37396794	*1030.24*	213.3349643
1040.09	410.8624577	253.4213368	*1043.51*	151.4882373	*1040.26*	368.4556968
1050.10	558.6637253	132.281373	*1053.11*	206.8744324	*1050.27*	335.3047203
1060.11	366.475188	70.4138447	*1062.70*	197.7358421	*1060.29*	342.982734
1070.11	243.3901684	−89.81088982	*1072.29*	44.39081555	*1070.30*	337.2164587
1080.12	−115.2303522	−410.9955609	*1081.87*	−71.0510886	*1080.32*	255.8050587
1090.13	−513.7217052	−673.9549008	*1091.45*	−144.2378713	*1090.33*	60.78419766

Table A1. *Cont.*

Leaf Level			Modeled Canopy		Measured Stand-Level Canopy	
Wavelength	**Leaf Reflectance**	**Leaf Tranmittance**	**Wavelength**	**Canopy Reflectance**	**Wavelength**	**Canopy Reflectance**
1100.13	−503.3266623	−735.2226782	*1101.02*	−175.982708	*1100.35*	−80.1777783
1110.14	185.6157309	-256.084212	*1110.59*	44.64300286	*1110.36*	−118.7303193
1120.15	824.8568883	474.0861467	*1120.15*	−79.57209073	*1120.38*	−30.42124311
1130.15	706.7412998	631.9688998	*1129.71*	73.0245519	*1130.39*	132.0979241
1140.16	−47.76023732	−114.2367884	*1139.26*	220.0080285	*1140.41*	124.772645
1150.17	−793.9397966	−1198.363214	*1148.81*	146.2877695	*1150.42*	158.8058648
1160.17	−745.6708347	−1504.678781	*1158.35*	31.91104367	*1160.44*	136.1227516
1170.18	−287.3397315	−977.1440687	*1167.88*	−142.3016634	*1170.45*	105.533777
1180.19	45.39977768	−275.292423	*1177.42*	−65.13435609	*1180.47*	−198.6871093
1190.19	26.74717705	211.8166676	*1186.94*	−91.04540926	*1190.48*	−245.5642678
1200.20	329.1118015	629.4019605	*1196.46*	145.3901957	*1200.50*	−248.8492534
1210.21	743.5419947	984.940179	*1205.98*	138.8085743	*1210.51*	−166.1981497
1220.21	806.117307	1071.042637	*1215.49*	164.0774127	*1220.53*	−150.0366876
1230.22	457.2073627	737.3979868	*1224.99*	271.7640207	*1230.54*	−213.122067
1240.23	−142.0063448	330.0453206	*1234.49*	39.18163026	*1240.56*	−187.9744947
1250.23	−543.5563157	146.9869822	*1243.99*	150.5001931	*1250.57*	−163.8988272
1260.24	−567.1012887	122.7306737	*1253.47*	26.67041061	*1260.59*	−140.5466685
1270.25	−264.606581	143.0742552	*1263.34*	−4.733391691	*1270.60*	−96.02582255
1280.25	−184.7943348	95.37154226	*1273.31*	−191.5538135	*1280.62*	−42.15363218
1290.26	−180.8847637	73.07818472	*1283.29*	−290.6901333	*1290.63*	−10.26607101
1300.26	−90.07775773	131.1229029	*1293.26*	−98.22080264	*1300.65*	36.6212788
1310.27	90.20361037	309.6023981	*1303.23*	−43.45230966	*1310.66*	31.15060269
1320.28	161.8813349	178.7665172	*1313.20*	29.02486545	*1320.68*	−16.79817654
1330.28	825.7565913	−351.9536778	*1323.17*	−127.8674268	*1330.69*	−70.6390652
1430.35	1217.506187	410.0379124	*1333.14*	−340.90711	*1430.84*	−24.89417885
1440.36	364.840675	−14.80275979	*1343.11*	−428.3056273	*1440.86*	−49.96475033
1450.36	−658.4000286	−584.856631	*1353.08*	802.2520087	*1450.87*	−119.3043298
1460.37	−1355.94315	−1006.842005	*1412.90*	18.45498708	*1460.89*	−174.8554044
1470.38	−1252.940641	−960.0889356	*1422.87*	−80.83907119	*1470.90*	−157.0907678
1480.38	−533.9116164	−424.473693	*1432.84*	−6.09757958	*1480.92*	−147.3426524
1490.39	387.0788578	197.1282446	*1442.81*	75.09399044	*1490.93*	−171.8612035
1500.40	933.0515097	607.9026065	*1452.78*	−64.0492756	*1500.95*	−173.3175564
1510.40	1031.005246	754.8906859	*1462.75*	−35.34963376	*1510.96*	−180.1370826
1520.41	639.7832858	706.9938317	*1472.71*	−63.16887986	*1520.98*	−157.4391749
1530.42	96.34347324	574.9548229	*1482.68*	−50.80736506	*1530.99*	−136.987365
1540.42	−189.0654619	392.9730658	*1492.65*	−98.97882395	*1541.01*	−115.2314186
1550.43	−361.200949	161.7731701	*1502.61*	−73.98580537	*1551.02*	−96.66156239
1560.44	−178.6693632	154.998368	*1512.58*	−71.04244606	*1561.04*	−83.42409227
1570.44	342.3061289	322.9407104	*1522.55*	120.6116297	*1571.05*	−78.92745713
1580.45	967.4233718	535.4395096	*1532.51*	115.2604483	*1581.07*	−64.5684128
1590.46	1169.502603	487.4268145	*1542.48*	97.45948869	*1591.08*	−57.98930307

Table A1. *Cont.*

Leaf Level			Modeled Canopy		Measured Stand-Level Canopy	
Wavelength	**Leaf Reflectance**	**Leaf Tranmittance**	**Wavelength**	**Canopy Reflectance**	**Wavelength**	**Canopy Reflectance**
1600.46	418.0703692	11.643117	*1552.44*	344.4234532	*1601.10*	−52.29878334
1610.47	−758.7646897	−737.6646856	*1562.41*	297.8169922	*1611.11*	−43.22761703
1620.48	−1458.921038	−1435.475427	*1572.38*	147.228783	*1621.13*	−34.71773851
1630.48	−1282.885825	−1632.853563	*1582.34*	−3.979286894	*1631.14*	−21.00074229
1640.49	−354.9454306	−1204.468722	*1592.31*	−67.83980097	*1641.16*	−8.324176442
1650.50	606.0061873	−278.1329802	*1602.27*	−117.3975702	*1651.17*	8.533159176
1660.50	812.9604732	722.4125758	*1612.23*	−153.6002936	*1661.19*	29.78949512
1670.51	340.5055387	1212.004563	*1622.20*	−186.0518129	*1671.20*	43.24976141
1680.52	−147.7023668	551.7746707	*1632.16*	−31.94937486	*1681.22*	39.1366824
1690.52	−721.3004094	−782.8080637	*1642.13*	−88.37862942	*1691.23*	28.98373127
1700.53	−1063.956987	−1701.277706	*1652.09*	71.4347783	*1701.25*	28.32998623
1710.54	−1021.160996	−1411.708312	*1662.05*	−35.17241089	*1711.26*	42.20150165
1720.54	6.498375354	−159.7847524	*1672.02*	153.8420071	*1721.28*	50.44622904
1730.55	1506.761755	934.7928816	*1681.98*	17.02008587	*1731.29*	48.67695955
1740.56	2001.84034	1247.12711	*1691.94*	11.48737073	*1741.31*	35.38533728
1750.56	792.8495698	800.840925	*1701.90*	−117.224093	*1751.32*	30.12835599
1760.57	−1214.787386	198.8604001	*1711.86*	−23.92446225	*1761.34*	33.86405036
1770.57	−1624.124566	13.98091789	*1721.83*	−118.81257	*1771.35*	39.34287819
2002.03	1468.02985	674.0373373	*1731.79*	−81.48569054	*2031.74*	−168.1982397
2012.03	561.4831546	1043.239315	*1741.75*	−133.9368218	*2041.76*	−256.4353296
2022.04	279.1126833	865.0245138	*1751.71*	−53.68955725	*2051.77*	−229.4068848
2032.05	288.9162004	465.6398897	*1761.67*	−222.5379453	*2061.79*	−216.1085252
2042.05	354.8780561	−322.9279525	*1771.63*	−89.06561924	*2071.80*	−116.234245
2052.06	−725.8204573	−863.3993494	*2028.37*	−41.38642304	*2081.82*	−82.83329552
2062.07	−1045.147746	−1199.012465	*2038.39*	39.6466759	*2091.83*	−71.22483251
2072.07	−1428.854761	−1392.963567	*2048.41*	−95.08716004	*2101.85*	−10.03137133
2082.08	−1066.911147	−1319.985558	*2058.43*	−122.4432577	*2111.86*	19.73794294
2092.09	−887.5673094	−616.6957406	*2068.45*	−173.3457587	*2121.88*	63.42453466
2102.09	−168.1844618	13.93939541	*2078.47*	−146.0312626	*2131.89*	80.01748509
2112.10	570.8179091	377.0661637	*2088.48*	−186.4526505	*2141.91*	90.98833299
2122.11	1261.525272	778.0295598	*2098.49*	−121.0580986	*2151.92*	105.7272038
2132.11	632.3631569	1161.737757	*2108.50*	22.81176134	*2161.94*	90.38333754
2142.12	574.7187805	639.1347964	*2118.51*	143.1007464	*2171.95*	86.59749841
2152.13	76.11790917	300.9941378	*2128.51*	99.37593363	*2181.97*	84.96181125
2162.13	92.69434539	249.2110435	*2138.51*	237.8748109	*2191.98*	67.64734018
2172.14	187.1006467	202.7932003	*2148.51*	229.0735066	*2202.00*	84.13533845
2182.15	748.6399275	246.9787361	*2158.51*	241.1260374	*2212.01*	64.51645446
2192.15	−553.2831637	38.50347028	*2168.50*	29.29752352	*2222.03*	59.6410842
2202.16	−734.7175539	−324.3644638	*2178.49*	−65.01128874	*2232.04*	70.06912197
2212.17	−676.6531445	−1061.113818	*2188.48*	−92.03031921	*2242.06*	81.06354185
2222.17	−982.810843	−832.2084714	*2198.47*	−126.5817693	*2252.07*	85.00666516
2232.18	−125.3762175	−609.0033076	*2208.46*	−79.10724312	*2262.09*	86.68867079

Table A1. *Cont.*

Leaf Level			Modeled Canopy		Measured Stand-Level Canopy	
Wavelength	Leaf Reflectance	Leaf Tranmittance	Wavelength	Canopy Reflectance	Wavelength	Canopy Reflectance
2242.19	241.835186	115.1755888	*2218.44*	−18.02558741	*2272.10*	78.18181046
2252.19	677.1287016	853.9901956	*2228.42*	15.19592898	*2282.12*	52.34591433
2262.20	1385.449441	1827.592724	*2238.40*	111.3126661	*2292.13*	85.49341794
2272.21	1337.826506	1569.501124	*2248.38*	212.2097671	*2302.15*	92.49323279
2282.21	−88.74063332	312.4205493	*2258.35*	148.0641274	*2312.16*	92.68125205
2292.22	−281.2954724	−722.3030813	*2268.32*	70.3796506	*2322.18*	126.3079726
2302.22	−1100.754704	−1959.00414	*2278.29*	−11.2907835	*2332.19*	87.48525986
2312.23	−1993.553061	−1621.390453	*2288.26*	138.9993526	*2342.21*	160.0424631
2322.24	−252.8753957	−1111.049991	*2298.22*	94.41060687	*2352.22*	216.9693838
2332.24	−114.6922794	−390.7161921	*2308.18*	8.420567335	*2362.24*	108.0718521
2342.25	1007.151283	124.2526096	*2318.14*	−57.95639111	*2372.25*	198.6993561
2352.26	186.6086765	818.4063019	*2328.10*	−89.67518112	*2382.27*	308.5381347
2362.26	368.286122	1228.437516	*2338.06*	166.1435471	*2392.28*	233.3352833
2372.27	1420.474875	1470.518086	*2348.01*	47.55116636	*2402.30*	199.913954
2382.28	−15.20402847	476.3402157	*2357.96*	−112.4039599	*2412.31*	328.566246
2392.28	487.8034804	875.0592421	*2367.91*	−92.34934375	*2422.33*	440.5182622
2402.29	−456.7426985	−67.04033764	*2377.86*	6.825447361	*2432.34*	228.0424133
2412.30	−761.5346907	−438.338257	*2387.80*	40.47869299	*2442.36*	180.3819973
2422.30	−716.306305	−951.80626	*2397.74*	115.8280977	*2452.37*	331.5718859
2432.31	19.14664416	−411.4209169	*2407.68*	−52.10616099	-	-
2442.32	87.46256623	−390.2173155	*2417.62*	35.37923776	-	-
2452.32	176.0899746	237.4730638	*2427.55*	−117.2654779	-	-
-	-	-	*2437.48*	114.907234	-	-
-	-	-	*2447.41*	−32.57342231	-	-
-	-	-	*2457.34*	−42.84769343	-	-

Notes: These PLSR weightings are provided for reference purposes only. They should not be used in place of calibrations with other spectrometers. Spectral PLSR weightings are specific to the spectrometer used, including its wavelength range, spectral resolution, and signal-to-noise performance. Wavelength values are in nanometers (nm).

References

1. Hoch, G.; Richter, A.; Körner, C. Non-structural carbon compounds in temperate forest trees. *Plant. Cell. Environ.* **2003**, *26*, 1067–1081.
2. White, L.M. Carbohydrate reserves of grasses: A review. *J. Range Manag.* **1973**, *26*, 13–18.
3. Chapin, F.S.; Wardlaw, I.F. Effect of phosphorus deficiency on source-sink interactions between the flag leaf and developing grain in barley. *J. Exp. Bot.* **1988**, *39*, 165–177.
4. Würth, M.K.R.; Pelãez-Riedl, S.; Wright, S.J.; Körner, C. Non-structural carbohydrate pools in a tropical forest. *Oecologia* **2005**, *143*, 11–24.
5. Dietze, M.C.; Sala, A.; Carbone, M.S.; Czimczik, C.I.; Mantooth, J.A.; Richardson, A.D.; Vargas, R. Nonstructural carbon in woody plants. *Ann. Rev. Plant. Biol.* **2014**, *65*, 667–687.

6. O'Brien, M.J.; Leuzinger, S.; Philipson, C.D.; Tay, J.; Hector, A. Drought survival of tropical tree seedlings enhanced by non-structural carbohydrate levels. *Nature Clim. Change* **2014**, *4*, 710–714.
7. Malhi, Y.; Aragão, L.E.O.C.; Galbraith, D.; Huntingford, C.; Fisher, R.; Zelazowski, P.; Sitch, S.; McSweeney, C.; Meir, P. Exploring the likelihood and mechanism of a climate-change-induced dieback of the amazon rainforest. *Proc. National Acad. Sci.* **2009**, *106*, 20610–20615.
8. Nepstad, D.; Lefebvre, P.; Da Silva, U.L.; Tomasella, J.; Schlesinger, P.; Solorzano, L.; Moutinho, P.; Ray, D.; Benito, J.G. Amazon drought and its implications for forest flammability and tree growth: A basin-wide analysis. *Glb. Change Biol.* **2004**, *10*, 704–717.
9. O'Brien, M.J.; Burslem, D.F.R.P.; Caduff, A.; Tay, J.; Hector, A. Contrasting nonstructural carbohydrate dynamics of tropical tree seedlings under water deficit and variability. *New Phytol.* **2014**, *205*, 1083–1094.
10. Asner, G.P.; Martin, R.E.; Tupayachi, R.; Anderson, C.B.; Sinca, F.; Carranza-Jimenez, L.; Martinez, P. Amazonian functional diversity from forest canopy chemical assembly. *Proc. National Acad. Sci.* **2014**, *111*, 5604–5609.
11. Asner, G.P.; Martin, R.E.; Anderson, C.B.; Knapp, D.E. Quantifying forest canopy traits: Imaging spectroscopy *versus* field survey. *Remote Sens. Environ.* **2015**, *158*, 15–27.
12. Kokaly, R.F.; Asner, G.P.; Ollinger, S.V.; Martin, M.E.; Wessman, C.A. Characterizing canopy biochemistry from imaging spectroscopy and its application to ecosystem studies. *Remote Sens. Environ.* **2009**, *113*, S78–S91.
13. Ustin, S.L.; Roberts, D.A.; Gamon, J.A.; Asner, G.P.; Green, R.O. Using imaging spectroscopy to study ecosystem processes and properties. *Bioscience* **2004**, *54*, 523–534.
14. Curran, P.J. Remote sensing of foliar chemistry. *Remote Sens. Environ.* **1989**, *30*, 271–278.
15. Asner, G.P. Biophysical remote sensing signatures of arid and semi-arid regions. In *Remote Sensing for Natural Resources, Management and Environmental Monitoring: Manual of Remote Sensing*; Ustin, S.L., Ed.; Wiley & Sons: New York, NY, USA, 2004; Vol. 4, pp. 53–109.
16. Asner, G.P.; Martin, R.E.; Knapp, D.E.; Tupayachi, R.; Anderson, C.; Carranza, L.; Martinez, P.; Houcheime, M.; Sinca, F.; Weiss, P. Spectroscopy of canopy chemicals in humid tropical forests. *Remote Sens. Environ.* **2011**, *115*, 3587–3598.
17. Asner, G.P.; Martin, R.E. Spectral and chemical analysis of tropical forests: Scaling from leaf to canopy levels. *Remote Sens. Environ.* **2008**, *112*, 3958–3970.
18. Jacquemoud, S.; Verhoef, W.; Baret, F.; Bacour, C.; Zarco-Tejada, P.J.; Asner, G.P.; Francois, C.; Ustin, S.L. Prospect plus sail models: A review of use for vegetation characterization. *Remote Sens. Environ.* **2009**, *113*, S56–S66.
19. Feret, J.-B.; Francois, C.; Asner, G.P.; Gitelson, A.A.; Martin, R.E.; Bidel, L.P.R.; Ustin, S.L.; le Maire, G.; Jacquemoud, S. Prospect-4 and 5: Advances in the leaf optical properties model separating photosynthetic pigments. *Remote Sens. Environ.* **2008**, doi:10.1016/j.rse.2008.02.012.
20. Verhoef, W.; Bach, H. Coupled soil-leaf-canopy and atmosphere radiative transfer modeling to simulate hyperspectral multi-angular surface reflectance and toa radiance data. *Remote Sens. Environ.* **2007**, *109*, 166–182.
21. Asner, G.P.; Martin, R.E. Canopy phylogenetic, chemical and spectral assembly in a lowland amazonian forest. *New Phytol.* **2011**, *189*, 999–1012.

22. Scurlock, J.M.O.; Asner, G.P.; Gower, S.T. *Worldwide Historical Estimates and Bibliography of Leaf Area Index, 1932–2000*; ORNL Technical Memorandum, TM-2001/268; Oak Ridge National Laboratory: Oak Ridge, TN, USA, 2001.
23. Asner, G.P.; Scurlock, J.M.O.; Hicke, J.A. Global synthesis of leaf area index observations: Implications for ecological and remote sensing studies. *Glb. Ecol. Biogeogr.* **2003**, *12*, 191–205.
24. Asner, G.P.; Knapp, D.E.; Boardman, J.; Green, R.O.; Kennedy-Bowdoin, T.; Eastwood, M.; Martin, R.E.; Anderson, C.; Field, C.B. Carnegie airborne observatory-2: Increasing science data dimensionality via high-fidelity multi-sensor fusion. *Remote Sens. Environ.* **2012**, *124*, 454–465.
25. Colgan, M.; Baldeck, C.; Féret, J.-B.; Asner, G. Mapping savanna tree species at ecosystem scales using support vector machine classification and brdf correction on airborne hyperspectral and lidar data. *Remote Sens.* **2012**, *4*, 3462–3480.
26. Haaland, D.M.; Thomas, E.V. Partial least-squares methods for spectral analyses. 1. Relation to other quantitative calibration methods and the extraction of qualitative information. *Anal. Chem.* **1988**, *60*, 1193–1202.
27. Gao, B.-C.; Goetz, A.F.H. Retrieval of equivalent water thickness and information related to biochemical components of vegetation canopies from aviris data. *Remote Sens. Environ.* **1995**, *52*, 155–162.
28. Chen, S.; Hong, X.; Harris, C.J.; Sharkey, P.M. Sparse modeling using orthogonal forest regression with press statistic and regularization. *IEEE Trans. Syst. Man Cybern.* **2004**, *34*, 898–911.
29. Sims, D.A.; Gamon, J.A. Relationships between leaf pigment content and spectral reflectance across a wide range of species, leaf structures and developmental stages. *Remote Sens. Environ.* **2002**, *81*, 337–354.
30. Curran, P.J.; Dungan, J.L.; Macler, B.A.; Plummer, S.E.; Peterson, D.L. Reflectance spectroscopy of fresh whole leaves for the estimation of chemical concentration. *Remote Sens. Environ.* **1992**, *39*, 153–166.
31. Vogelmann, T.C.; Nishio, J.N.; Smith, W.K. Leaves and light capture: Light propagation and gradients of carbon fixation within leaves. *Trends Plant. Sci.* **1996**, *1*, 65–70.
32. Roberts, D.A.; Nelson, B.W.; Adams, J.B.; Palmer, F. Spectral changes with leaf aging in Amazon caatinga. *Trees* **1998**, *12*, 315–325.
33. Ollinger, S.V. Sources of variability in canopy reflectance and the convergent properties of plants. *New Phytol.* **2011**, *189*, 375–394.
34. Asner, G.P. Biophysical and biochemical sources of variability in canopy reflectance. *Remote Sens. Environ.* **1998**, *64*, 234–253.
35. Jacquemoud, S.; Baret, F. Prospect—A model of leaf optical-properties spectra. *Remote Sens. Environ.* **1990**, *34*, 75–91.
36. Martin, M.E.; Plourde, L.C.; Ollinger, S.V.; Smith, M.-L.; McNeil, B.E. A generalizable method for remote sensing of canopy nitrogen across a wide range of forest ecosystems. *Remote Sens. Environ.* **2008**, *112*, 3511–3519.
37. Kerespi, I.; Toth, M.; Boross, L. Water-soluble carbohydrates in dried plant. *J. Agric. Food Chem.* **1996**, *44*, 3235–3239.

38. Doughty, C.E.; Goulden, M.L. Seasonal patterns of tropical forest leaf area index and CO_2 exchange. *J. Geophys. Res.* **2008**, *113*, doi:10.1029/2007JG000590.
39. Wessman, C.A.; Aber, J.D.; Peterson, D.L.; Melillo, J.M. Foliar analysis using near infrared reflectance spectroscopy. *Can. J. For. Res.* **1988**, *18*, 6–11.
40. Knyazikhin, Y.; Schull, M.A.; Stenberg, P.; Mõttus, M.; Rautiainen, M.; Yang, Y.; Marshak, A.; Latorre Carmona, P.; Kaufmann, R.K.; Lewis, P.; *et al.* Hyperspectral remote sensing of foliar nitrogen content. *Proc. Natl. Acad. Sci.* **2013**, *110*, E185–E192.
41. Aber, J.D.; Melillo, J.M. *Terrestrial Ecosystems*; Saunders College Publishing: Philadephia, PA, USA, 1991; p. 429.